ELSEVIER

Journal of Molecular Catalysis A: Chemical 175 (2001) 241–248

JOURNAL OF MOLECULAR CATALYSIS A: CHEMICAL

www.elsevier.com/locate/molcata

Investigations of nitric oxide and carbon monoxide adsorption on the new generation cerium exchanged silico-aluminophosphate of type 18 catalyst

Chris Kladis [a], Suresh K. Bhargava [a,*], Karl Foger [b], Deepak B. Akolekar [a]

[a] *Department of Applied Chemistry, Materials Research Group, RMIT University, City campus, Melbourne, Vic. 3001, Australia*
[b] *Ceramic Fuel Cells Limited, 170 Browns Road, Noble Park, Vic. 3174, Australia*

Received 16 March 2001; received in revised form 18 April 2001; accepted 8 May 2001

Abstract

Cerium exchanged SAPO-18 material showed adsorptivity for NO and CO molecules. In situ adsorption of nitric oxide and carbon monoxide on cerium exchanged SAPO-18 materials was studied by FT-IR spectroscopy. The cerium exchanged SAPO-18 samples were prepared using the highly crystalline and pure H-SAPO-18 material. The SAPO-18 and cerium exchanged SAPO-18 materials were characterised by routine and sophisticated instrumental techniques. The presence of both Ce^{III} and Ce^{IV} species on the surface of the Ce-SAPO-18 catalyst were revealed by the XPS technique. The concentration of cerium is higher on the surface of the material than in the bulk. The interaction of NO with Ce-SAPO-18 material led to the formation of nitrous oxide, mono- and di-nitrosyl complexes of cerium, nitrogen dioxide and nitrate species. The formation of mono-, di- and tri- carbonyl complexes of cerium and carbon dioxide species were observed after the carbon monoxide adsorption on the Ce-SAPO-18.

Keywords: XPS; Surface species; NO; CO; Ce-SAPO-18; FT-IR; SAPO-18; Silico-aluminophosphates

1. Introduction

The interaction of nitric oxide and carbon monoxide with metal oxide surfaces has been extensively studied by the ways of adsorption and catalytic decomposition methods on the noble metals and modified zeolites. Cerium oxide, which is one of the important components of automotive and industrial exhaust catalyst, is active for NO_x removal, oxidation of CO and hydrocarbons and hydrogenation as well acts as oxygen storage in the lattice of cerium oxide [1–6]. The surface area and the type of active sites/species are important factors in the deciding the catalytic activity of material. Because, of the limitations in increasing the surface area of cerium oxide, a high surface cerium containing novel catalytic material using a cerium compound and silico-aluminophosphate (SAPO-*n*) type molecular sieve has been developed. SAPO-*n* are new type of materials which exhibit mild to strong acidity, catalytic activity, ion-exchange capacity, framework flexibility and cation-exchange properties as a result of the isomorphous substitution of P in $AlPO_4$ by Si [7–12]. The metal exchanged SAPO-*n* material possesses excellent thermostable characteristics and high surface area. Recently, similar materials have been utilised for the decomposition of NO_x

* Corresponding author. Tel.: +61-3-99253365; fax: +61-3-96391321.
E-mail address: suresh.bhargava@rmit.edu.au (S.K. Bhargava).

1381-1169/01/$ – see front matter
PII: S1381-1169(01)00224-2

[13,14]. The purpose of this study is to examine the nature of active sites on the cerium exchanged SAPO material. The nature of active metal sites is usually studied with nitric oxide [14–17] or carbon monoxide [16–19] probe molecules using the FT-IR technique. In the present paper, the adsorption-interaction of NO and CO molecules with the active cerium species on the modified crystalline silico-aluminophosphate of type 18 (SAPO-18) catalyst was investigated.

2. Experimental

Ce-SAPO-18 was prepared by the liquid ion-exchange method [17,18]. The calcined SAPO-18 was ion-exchanged with Ce in 0.010 M cerium nitrate solution at 343 K for 2 h, then filtered, washed and dried. The ion-exchange procedure was repeated twice. The Ce-SAPO-18 was dried overnight at 373 K and then heated at 773 K for 5 h. SAPO-18 was obtained by calcination of the as-synthesised SAPO-18. As-synthesised SAPO-18 was prepared by hydrothermal crystallisation of gel (molar composition: 1.6 $C_8H_{19}N$; 1.0 Al_2O_3; 0.4 SiO_2; 0.9 P_2O_5; 50 H_2O) in a Teflon-lined stainless steel autoclave at 443 K for 8 days [20]. The crystallisation product was filtered, thoroughly washed and dried in air at 343 K. The *N*,*N*-diisopropylethylamine template was removed by calcination in a muffle furnace at 773 K for 16 h. The chemicals used for the synthesis work were Catapal (aluminium oxyhydroxide), *o*-phosphoric acid (85%, Merck), Aerosil (fumed silica) and *N*,*N*-diisopropylethylamine (99%, Aldrich).

The materials were characterized by elemental analysis, XRD, SEM, BET and XPS techniques. The X-ray powder diffraction pattern of the as-synthesized SAPO-18 obtained with Philips PA2000 diffractometer. The chemical composition of the samples was determined by ICP-OES analysis (Perkin-Elmer Optima 3000 DV). The details of characterization techniques and instrument utilized for the chemical analysis and structure determination were reported earlier [8]. The surface area and pore volume of the materials were obtained by BET (N_2-dynamic adsorption/desorption) technique ($p/p_o = 0.3$) using a Micromeritics ASAP2000 Instrument. The morphology and crystal size of the materials were investigated using a JEOL JSM 35MF scanning electron microscope.

XPS surface analysis were conducted for determining the surface concentration and binding energy of O_{1s}, Si_{2p}, Al_{2p}, P_{2p} and Ce_{3d} using a Fisons system (operated in the constant pass energy mode of 20 eV). All spectra were referenced to C_{1s} (285 eV). An Mg Kα X-ray source ($h\nu = 1253.7$ eV) was operated at 20 mA and 15 mV. The base pressure of the instrument was 10^{-9} Torr. The intensity of the XPS band was determined using linear background subtraction and integration of peak areas. FT-IR studies were performed on self-supported wafers (ca. 20 mg, thickness of 10.0 mg cm^{-2}). A self-supported wafer was fixed to a stainless steel holder located in the sample holder of a Pyrex/quartz FT-IR cell. All samples were first activated under vacuum ($<10^{-4}$ Torr) at 573 K for 16 h. A high purity mixture of nitrogen (95%) and nitric oxide (5%) and carbon monoxide (99.95%) supplied by Linde, Australia were used as the NO or CO source. FT-IR spectra of the samples were obtained at 2 cm^{-1} resolution using a Perkin-Elmer System 2000 or 1725× FT-IR spectrometer. The spectrum of the dehydrated sample was used as a background from which the adsorbed spectrum was subtracted and necessary background subtractions were concluded for all the spectra. The FT-IR spectra were collected at 297.5 K and at different gas pressure (equilibrium depending upon the experimental conditions).

3. Results and discussion

The Ce-SAPO-18 catalyst was prepared from the highly crystalline and pure SAPO-18. The crystallite size of the SAPO-18 varied from 5–7 μm. The chemical composition and surface properties of the Ce-SAPO-18 catalyst are presented in Table 1. The observed surface area of the SAPO-18 was 653 m^2 g^{-1}. After the cerium exchange SAPO-18 material, decrease in the total surface area (by 37% from 653 to 414 m^2 g^{-1}) and the micropore volume (by 44% from 0.25 to 0.14 cm^3 g^{-1}) was observed. The decline in the total surface area and pore volume is due to pore blockage caused by cerium in the SAPO-18 structure [12]. Table 1 shows the surface concentration of the elements and the binding energy data for the Ce-SAPO-18 catalyst. The results of bulk chemical and XPS surface analysis of the Ce-SAPO-18 material indicates the concentrations of aluminium, silicon and

Table 1
Comparison of the physical and chemical properties of the SAPO-18 and Ce-SAPO-18

Product composition (mol%)	
SAPO-18 (calcined)	Si, 17.7; Al, 42.9; P, 39.4
Ce-SAPO-18	Ce, 5.5; Si, 16.7; Al, 40.6; P, 37.2
Surface area, micropore volume	
SAPO-18 ($m^2\,g^{-1}$)	653
SAPO-18 ($cm^3\,g^{-1}$)	0.25
Ce-SAPO-18 ($m^2\,g^{-1}$)	413
Ce-SAPO-18 ($cm^3\,g^{-1}$)	0.14
Surface composition (at.%)	Ce_{3d} 6.8; Si_{2p} 3.9; Al_{2p} 10.1; P_{2p} 14.5; O_{1s} 60.5; C_{1s} 4.2
E_b/eV (FWHM/eV)[a]	Ce^{III} 883; Ce^{IV} 886.3; Si_{2p} 102.1; Al_{2p} 75.1; P_{2p} 134.4; O_{1s} 532.2

[a] Referenced to C_{1s} (285 eV).

phosphorous are lower on the surface than in the bulk. The higher surface Ce/Al ratio (0.67) indicates that most of the Ce metal ions are present on the surface of the SAPO-18 molecular sieve. The observed binding energies 883 and 886 eV indicated the presence of both the Ce^{III} and Ce^{IV} species in the SAPO-18 catalyst. The binding energies (Table 1) of the other elements (Al_{2p}, Si_{2p} and P_{2p}) are close to those for tetrahedrally coordinated elements in metal substituted aluminophosphates [21] and low silica zeolites [22].

Figs. 1 and 2 show the NO adsorption on the Ce exchanged SAPO-18. After dehydration of Ce-SAPO-18 in vacuo at 573 K for 16 h, exposure to NO produced up to four strong bands attributed to the formation of nitrous oxide, nitrogen dioxide, mono- and di-nitrosyl species. The NO adsorption (at 12 Torr) produced strong bands at 1912, 1834, 1741, and 2250–2150 cm^{-1} are assigned to Ce^{III}–NO, Ce^{III}–$(NO)_2$ (symmetric), Ce^{III}–$(NO)_2$ (asymmetric) and Ce^{IV}–N_2O adsorbed species, and very weak band at 1625 assigned to Ce^{IV}–NO_2, respectively. These band assignments are in good agreement with other published data [14–18,23–27]. The nitrosyl cerium complexes and intermediates resulting from surface reaction between nitric oxide and Ce-SAPO-18 are summarised in Table 2. NO adsorption experiments at various pressures and temperatures were carried out in order to study the influence of nitric oxide gas pressure on the cerium–nitric oxide complexes. FT-IR results pertaining to the pressure changes of NO on the Ce-SAPO-18 are presented in Fig. 1. At a pressure of 12 Torr NO gas shows the appearance of both mononitrosyl and dinitrosyl bands. When 22 Torr of NO gas is introduced into the cell, the intensity of the mononitrosyl increases and that of the dinitrosyl decreases with large amount formation of Ce^{IV}–NO_2 and Ce^{IV}–N_2O. After 61 Torr of NO gas is added, it appears that the dinitrosyl Ce^{III} complex subsequently is oxidized and converts to an unstable Ce^{IV} complex with N_2O and O^- adsorbed species and a decrease in presence of the Ce^{IV}–NO_2 species. Further reaction with NO at higher pressure (72 Torr) sees the conversion of the unstable N_2O and O^- complex to the Ce^{IV}–NO_2 species, while the levels of Ce^{III}–NO and Ce^{III}–$(NO)_2$ remain more or less similar to that of NO pressure at 61 Torr [15,28–30]. The above results would indicate that some sort of dual mechanism could be involved. The first mechanism proposed involves the direct conversion of the Ce^{III}–NO specie to the Ce^{IV}–NO_2 specie via the Ce^{III}–$(NO)_2$ specie. This direct conversion is caused by the higher concentration of cerium on the surface of the material. The second mechanism involves the well documented conversion of Ce^{III}–NO specie to the Ce^{IV}–NO_2

Table 2
Assignment of the type of species generated after the interaction of NO and CO with the cerium exchanged SAPO-18 catalyst

Species	Wavenumber (cm^{-1})
Ce^{III}–NO	1912
Ce^{III}–$(NO)_2$ (symmetric)	1843
Ce^{III}–$(NO)_2$ (asymmetric)	1739
Ce^{IV}–NO_2	1625
Ce^{IV}–N_2O	2250–2150
Ce^{III}–CO	2117
Ce^{III}–$(CO)_2$ (symmetric)	2174
Ce^{IV}–CO_2	1620

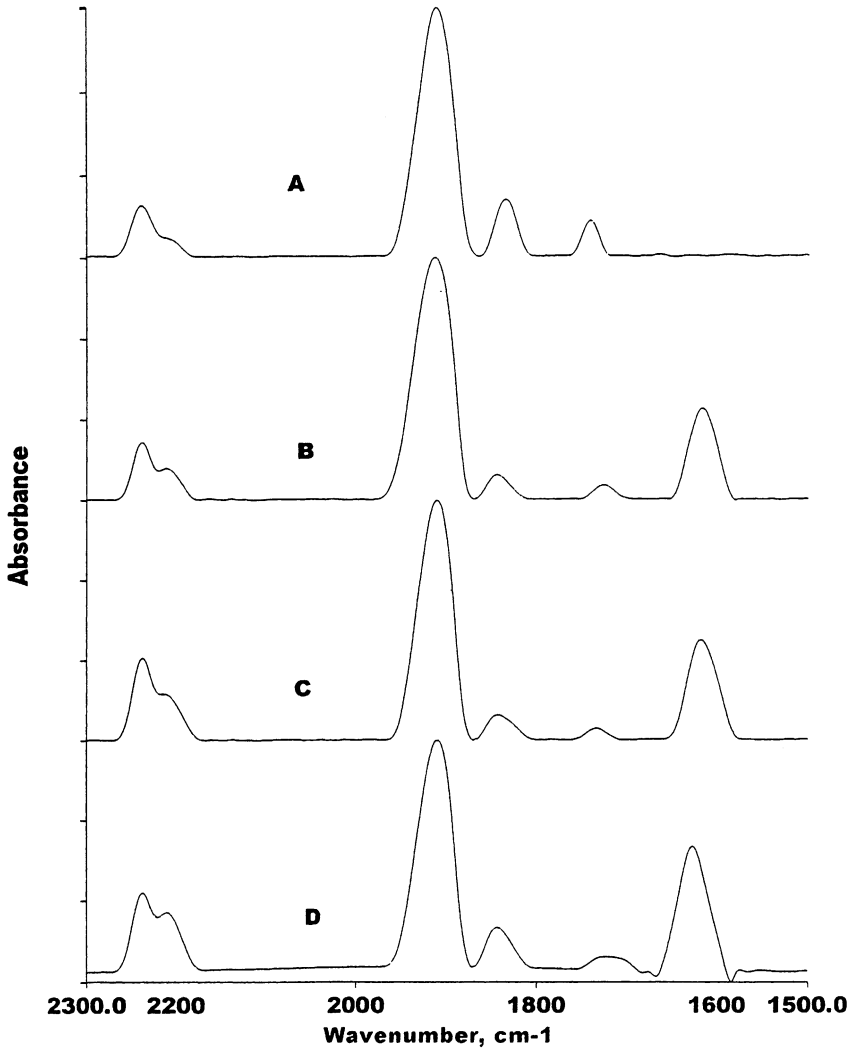

Fig. 1. FT-IR spectrum of NO adsorbed at 297.5 K and at various pressures over the dehydrated Ce-SAPO-18 catalyst: (A) 12; (B) 22; (C) 61; and (D) 72 Torr.

specie via the Ce^{III}–$(NO)_2$ and unstable Ce^{IV}–N_2O species [14–18].

The decomposition of adsorbed NO species at different temperatures and constant pressure over the dehydrated Ce-SAPO-18 catalyst is shown in Fig. 2. The investigation was undertaken at a NO pressure of 32 Torr and temperatures of 303, 373 and 473 K for 30 min. NO adsorption pressure of 32 Torr shows the appearance of major bands at 1914, 1836, 1743, 1621 and 2250–2150 cm^{-1} are assigned to Ce^{III}–NO, Ce^{III}–$(NO)_2$ (symmetric), Ce^{III}–$(NO)_2$ (asymmetric), Ce^{IV}–NO_2 and Ce^{IV}–N_2O adsorbed species. At a temperature of 373 K, the intensity of the Ce^{III}–NO band decreased while the intensity of the Ce^{IV}–NO_2 band remained the same but a new Ce^{IV}–NO_3 complex formed indicating the decomposition of Ce^{III}–NO to Ce^{IV}–NO_2 and Ce^{IV}–NO_3 (at 1564 cm^{-1}). The concentration of Ce^{IV}–N_2O species was increased at the reaction temperature of 373 K. Further at 473 K, the Ce^{IV}–NO_3 complex formation was enhanced as observed by the increase in the peak intensity at 1564 while the Ce^{IV}–NO_2 complex diminished (1.5:1 ratio

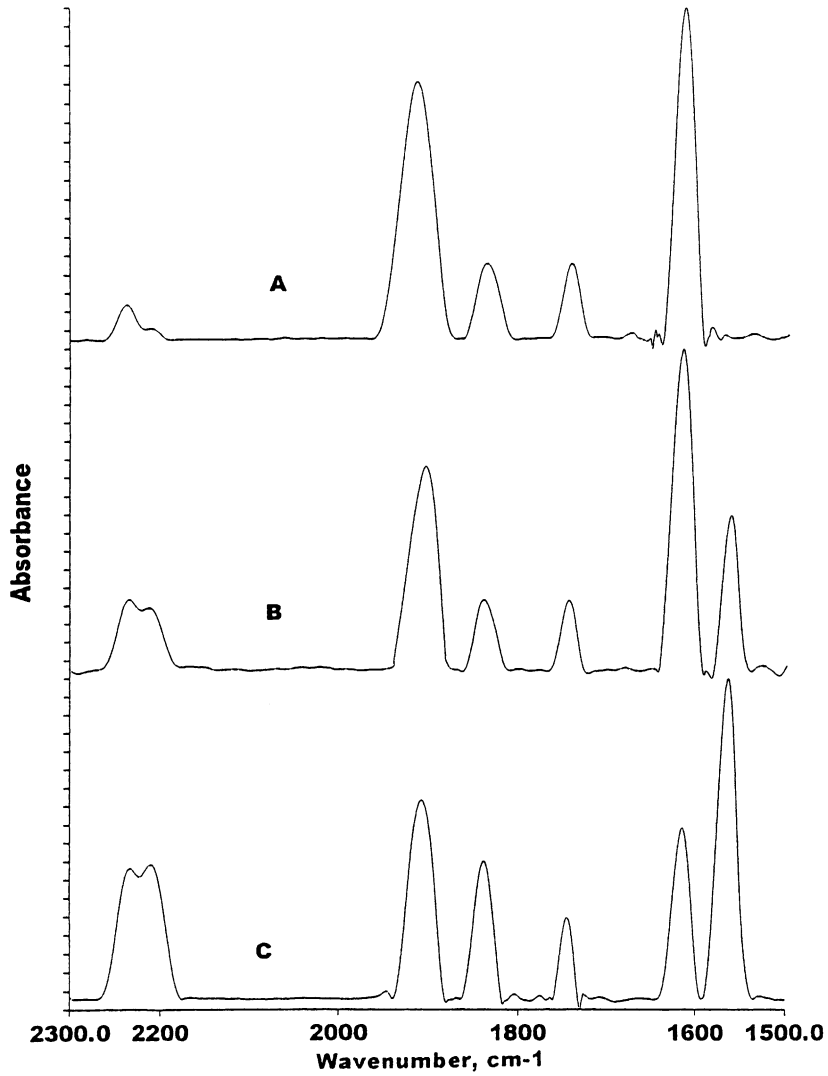

Fig. 2. FT-IR spectrum of NO adsorbed at constant pressure and different temperatures over the dehydrated Ce-SAPO-18 catalyst: (A) 32 Torr, 303 K; (B) 32 Torr, 373 K; (C) 32 Torr, 473 K.

of intensity). The significant increase in the formation of Ce^{IV}–N_2O was observed at the higher reaction temperature (473 K) and the intensities of other bands were slightly increased. This indicates that at higher reaction temperature, the Ce^{IV}–NO_2 complex decomposes to a N_2O and O^- complex and to other species.

Figs. 3 and 4 show the CO adsorption on Ce-SAPO-18. After dehydration of Ce-SAPO-18 in vacuo at 573 K for 16 h, exposure to CO produced up to three strong bands attributed to the formation of carbon dioxide, mono-, di-carbonyl species. The bands at 2174 (strong), 2117 (strong), 2075 (shoulder), and 1618 (week) cm^{-1} are assigned to Ce^{III}–$(CO)_2$ (symmetric and asymmetric), Ce^{III}–CO, and Ce^{IV}–CO_2 adsorbed species, respectively. The band of Ce^{IV}–CO_2 adsorbed species is clearly visible at high CO pressures. These band assignments are in good agreement with other published data

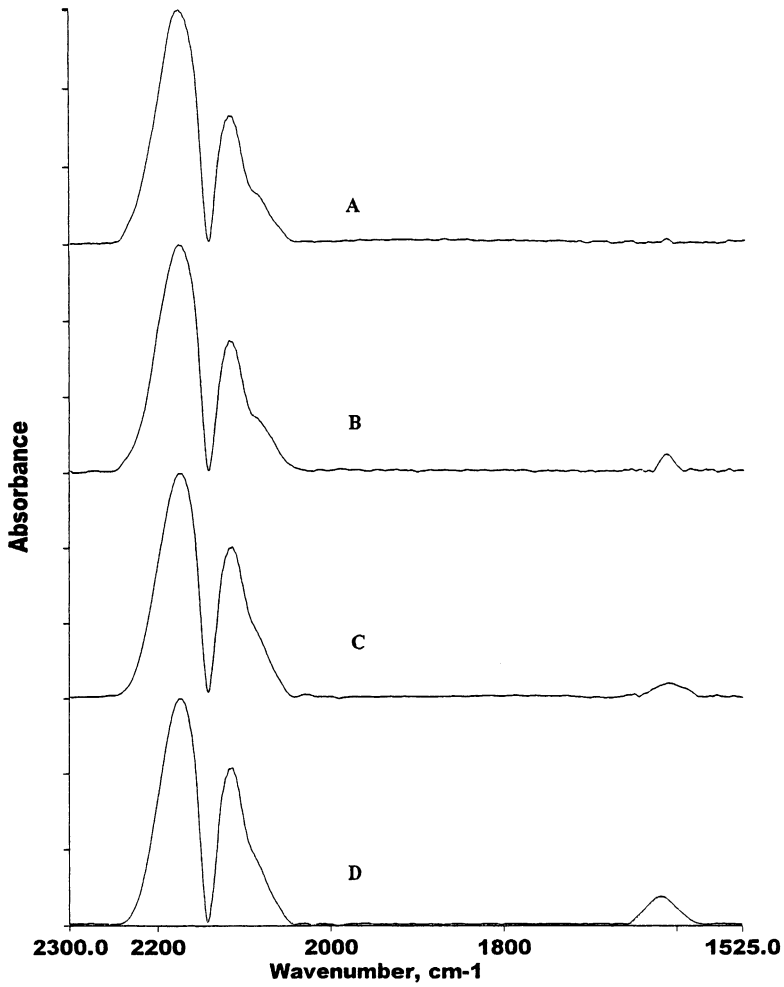

Fig. 3. FT-IR spectrum of CO adsorbed at 297.5 K and at various pressures and constant temperature over the dehydrated Ce-SAPO -18 catalyst: (A) 12; (B) 22; (C) 61; and (D) 72 Torr.

[16,18,19,27,31]. Table 2 shows the carbonyl cerium complexes and intermediates resulting from surface reaction between carbon monoxide and Ce-SAPO-18. CO adsorption experiments at various pressures and temperatures were carried out in order to study the influence of carbon monoxide gas pressure on the cerium–carbon monoxide complexes. FT-IR results pertaining to the pressure changes of CO (at constant temperature) on Ce-SAPO-18 are presented in Fig. 3. A pressure of 12 Torr CO gas sees the appearance of both mono- and di-carbonyl bands as well as carbon dioxide. When 22 Torr of CO gas is introduced into the cell, the intensity of the Ce^{III}–CO, Ce^{IV}–CO_2 bands increases while that of Ce^{III}–$(CO)_2$ remains constant. The trend is similar for the CO adsorption pressures at 61 and 72 Torr. This indicates the cerium–carbonyl complexes are formed on the active sites of the SAPO-18 catalyst. It appears that the conversion of Ce^{III}–CO to Ce^{IV}–CO_2 would also follow a direct conversion mechanism similar to the one observed with Ce^{III}–NO to Ce^{IV}–NO_2. As with the nitric oxide system this phenomena can be attributed to the high cerium surface concentration. Fig. 4 shows the behavior of adsorbed CO species

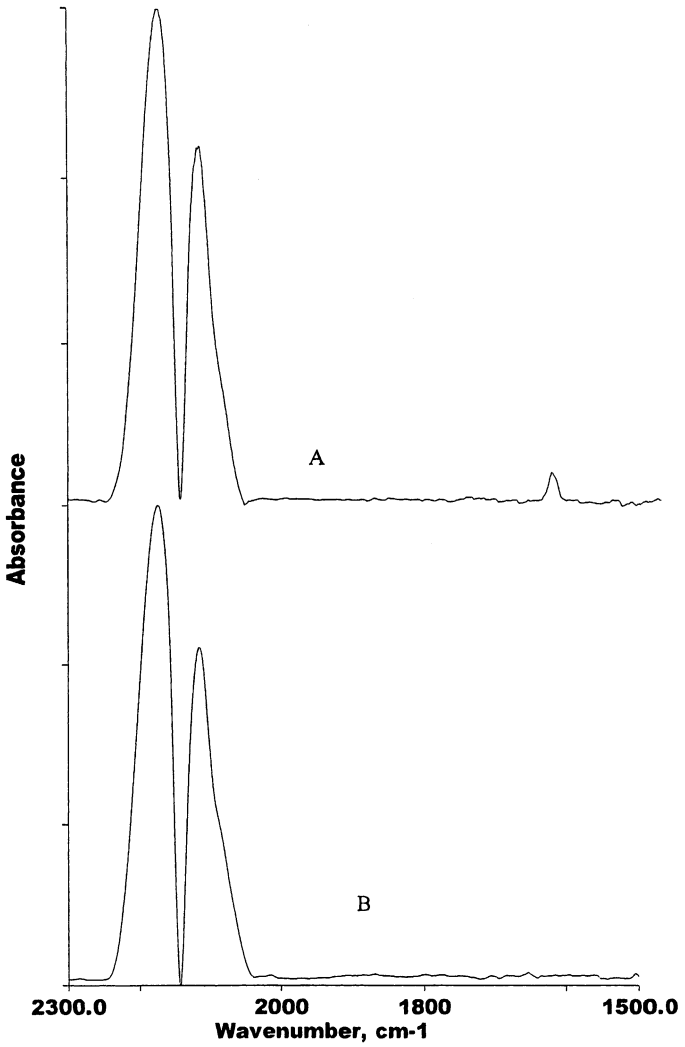

Fig. 4. FT-IR spectrum of CO adsorbed at constant pressure and different temperatures over the dehydrated Ce-SAPO-18 catalyst: (A) 26 Torr, 303 K; (B) 26 Torr, 473 K.

at 303 and 473 K temperatures and constant pressure over the dehydrated Ce-SAPO-18 catalyst. The investigation was undertaken at CO pressure of 26 Torr and temperatures of 373 and 473 K for 30 min. The FTIR results show that the band intensity of mono-carbonyl species decreases slightly and the Ce^{IV}–CO_2 band completely disappeared at 473 K temperature. This indicates that the Ce^{IV}–CO_2 complex decomposed to form the Ce^{III}–$(CO)_2$ and Ce^{III}–CO complexes. The high temperature ($\geq$473 K)) decomposition of adsorbed NO and CO over the dehydrated Ce-SAPO-18 catalyst shows that the concentrations of Ce^{IV}–NO_2 and Ce^{IV}–CO_2 species decreases as well as changes occur in the concentration of other species. On Ce-SAPO-18, the NO and CO sites are of similar type to those over the Cu-SAPO-34, Cu- and Ce-ZSM-5 catalysts. However, the observed concentration of Ce^{III}–NO and Ce^{III}–CO species were higher over the Ce-SAPO-18 than the Cu-SAPO-34 and Cu-ZSM-5 catalysts.

4. Conclusions

The adsorption of NO on the Ce-SAPO-18 catalyst resulted in the formation of Ce^{III}–NO, Ce^{III}–$(NO)_2$ (symmetric), Ce^{III}–$(NO)_2$ (asymmetric), Ce^{III}–N_2O and Ce^{IV}–NO_2 species. High temperature decomposed the Ce^{IV}–NO_2 complex to the Ce^{III}–N_2O, Ce^{III}–NO and Ce^{III}–$(NO)_2$ complexes. The adsorption of carbon monoxide on the Ce-SAPO-18 catalysts resulted in the formation of Ce^{III}–CO, Ce^{III}–$(CO)_2$, and Ce^{IV}–CO_2 species. The types of NO and CO sites on the catalysts are similar to those observed on the other metal exchanged microporous catalysts. XPS analysis revealed the presence of Ce^{III} and Ce^{IV} surface species and the higher surface concentration of Ce on the Ce-SAPO-18.

Acknowledgements

The authors would like to thank Dr. J. Gorman, Department of Applied Physics, RMIT University, Melbourne, Australia for assistance with the XPS analyses and Dr. C. Cunningham, Perkin-Elmer, Melbourne, Australia for assistance with the ICP-OES analyses.

References

[1] G. Li, K. Kaneko, S. Ozeki, Langmuir 13 (22) (1997) 5894.
[2] G. Bosca, V. Lorenzelli, J. Catal. 72 (1981) 303.
[3] K. Kaneko, A. Matsumoto, J. Phys. Chem. 93 (1989) 8090.
[4] M. Niwa, Y. Furikawa, Y.J. Murakami, J. Colloid Interface Sci. 86 (1982) 260.
[5] M. Iwamoto, Stud. Surf. Sci. Catal. 84 (1994) 1395.
[6] M. Iwamoto, Chem. Lett. (1991) 1859.
[7] S.T. Wilson, B.M. Lock, E.M. Flanigen, US Patent No. 4310440 (1982).
[8] D.B. Akolekar, J. Catal. 144 (1993) 148.
[9] E.M. Flanigen, R.L. Patton, S.T. Wilson, Stud. Surf. Sci. Catal. 37 (1988) 13.
[10] G.J. Gajda, R.T. Gajek, US Patent No. 5723710 (1996).
[11] R.M. Barrer, Zeolites, Clay Minerals, Academic Press, London, 1978.
[12] D.W. Breck, Zeolite Molecular Sieves, Wiley, New York, 1974.
[13] T. Ishihara, M. Kagawa, F. Hadama, Y. Takita, Stud. Surf. Sci. Catal. 84 (1994) 1493.
[14] D.B. Akolekar, S.K. Bhargava, K. Foger, J. Chem. Soc. Faraday Trans. 94 (1998) 155.
[15] T. Cheung, S.K. Bhargava, M. Hobday, K. Foger, J. Catal. 158 (1996) 301.
[16] D.B. Akolekar, S.K. Bhargava, Stud. Surf. Sci. Catal. 105 (1998) 755.
[17] C. Kladis, S.K. Bhargava, D.B. Akolekar, K. Foger, Catal. Today 63 (2000) 297.
[18] C. Kladis, S.K. Bhargava, K. Foger, D.B. Akolekar, J. Mol. Catal., 2001, in press.
[19] K. Hadjiivanov, M. Kantcheva, D. Klissurski, J. Chem. Soc., Faraday Trans. 92 (1996) 4595.
[20] J. Chen, P. Wright, J.M. Thomas, S. Natarajan, L. Marchese, S. Bradley, G. Sankar, C. Richard, A. Catlow, P. Gai-Boyes, R. Townsend, M. Lok, J. Phys. Chem. 98 (1994) 10216.
[21] D.B. Akolekar, J. Catal. 143 (1993) 227.
[22] M. Huang, A. Adnot, S. Kaliaguine, J. Catal. 137 (1992) 322.
[23] E. Shpiro, R.W. Joyner, W. Grunert, N.W. Haynes, M.R.H. Siddiqui, G.N. Baeva, Stud. Surf. Sci. Catal. 84 (1994) 1483.
[24] T. Ishihara, M. Kagawa, F. Hadama, Y. Takita, J. Catal. 169 (1997) 93.
[25] M. Iwamoto, H. Yahiro, N. Mizuno, W.-X. Zhang, Y. Mine, H. Furukawa, S. Kagawa, J. Phys. Chem. 96 (1992) 9360.
[26] K.I. Hadjivanov, Catal. Rev.-Sci. Eng. 42 (1/2) (2000) 71.
[27] R. Keiski, M. Harkonen, A. Lahti, T. Maunula, A. Savimaki, T. Slotte, Stud. Surf. Sci. Catal. 96 (1995) 85.
[28] G. Spoto, S. Bordiga, D. Scarano, A. Zecchina, Catal. Lett. 13 (1992) 39.
[29] J. Valyon, W.K. Hall, J. Catal. 143 (1993) 520.
[30] J. Valyon, W.K. Hall, J. Phys. Chem. 97 (1993) 1204.
[31] T. Pieplu, F. Poignant, A. Vallet, J. Saussey, J.C. Lavalley, Stud. Surf. Sci. Catal. 96 (1995) 619.